Biochemical and Biophysical Research Communications **269,** 58–63 (2000)
doi:10.1006/bbrc.2000.2259, available online at http://www.idealibrary.com on IDEAL®

Engineering His(E7) Affects the Control of Heme Reactivity in *Aplysia limacina* Myoglobin

Luca Federici, Carmelinda Savino, Raffaella Musto, Carlo Travaglini-Allocatelli, Francesca Cutruzzolà, and Maurizio Brunori

Department of Biochemical Sciences "A. Rossi Fanelli" and C.N.R. Center for Molecular Biology, University of Rome "La Sapienza", Piazzale Aldo Moro 5, 00185 Rome, Italy

Received January 14, 2000

Aplysia limacina **myoglobin lacks the distal histidine (His (E7)) and displays a ligand stabilization mechanism based on Arg(E10). The double mutant Val(E7)His-Arg(E10)Thr has been prepared to engineer the role of His(E7), typical of mammalian myoglobins, in a different globin framework. The 2.0 Å crystal structure of Val(E7)His-Arg(E10)Thr met-Mb mutant reveals that the His(E7) side chain points out of the distal pocket, providing an explanation for the observed failure to stabilize the Fe(II) bound oxygen in the ferrous myoglobin. Moreover, spectroscopic analysis together with kinetic data on azide binding to met-myoglobin are reported and discussed in terms of the presence of a water molecule at coordination distance from the heme iron.** © 2000 Academic Press

The myoglobin (Mb) from the buccal muscle of the gastropod mollusc *Aplysia limacina* has been widely studied given the interesting and peculiar features of its ligand binding pocket. The 146 residues protein (1, 2) has a typical globin fold (3), despite the very limited sequence homology with other myoglobins, notably those from mammals. A distinctive feature is the presence of only one histidyl residue located at the proximal heme iron coordination position (His(F8)).[1] The distal histidine, which has been shown to play a major role in most vertebrate myoglobins (5, 6), is replaced by a valyl residue at the topological position E7. The active site reactivity of *A. limacina* Mb has been studied by equilibrium and kinetic methods on site-directed mutants (2). O_2 stabilization was suggested (7) to depend on interactions with Arg(E10), underlying a mechanism totally different from that characteristic of vertebrate Mbs. Substitution of Arg(E10) with Thr (2), is associated to an increase in the O_2 dissociation rate constant to $k_{off} \approx 700\ s^{-1}$, whereas in the native protein $k_{off} = 70\ s^{-1}$ (8); thus the role of Arg(E10) in O_2 stabilization in *A. limacina* Mb was proven. However the replacement of Val(E7) with His, in both the single mutant Val(E7)His and the double mutant Val(E7)His-Arg(E10)Thr, while lowering the very high O_2 dissociation rate observed with the single mutant Arg(E10)Thr, failed to reproduce the value typical of sperm whale Mb ($k_{off} = 15\ s^{-1}$; (9)).

In order to understand the structural basis for this puzzling observation whereby His(E7) in the *A. limacina* Mb framework does not stabilize bound O_2, we have solved the 2.0 Å resolution crystal structure of the double mutant Val(E7)His-Arg(E10)Thr *A. limacina* Mb in the ferric form. Together with new spectroscopic and kinetic data we can provide an explanation of the unexpected O_2 reactivity. First of all, we confirm dependence of the stabilization of the O_2 complex on the H-bonding capability of side chains in the distal pocket and the accessibility to the solvent of the ligand binding pocket. We provide direct evidence for the presence of a water molecule at coordination distance to the iron in the met form, as suggested by the optical spectrum of this mutant (2). Finally, to further investigate the ligand stabilization properties of His(E7) in this double mutant, we report data on azide binding, since this ligand of the ferric form is a useful probe of distal pocket stereochemistry and polarity and its binding to the heme iron involves displacement of the water molecule (if present) and interaction with the positive dipoles in the heme pocket (10).

MATERIALS AND METHODS

Crystallization and data collection. A. limacina recombinant double mutant Val(E7)His-Arg(E10)Thr (*Aply*HT-Mb) was purified as already described (2). The crystallization conditions used to crystallize the native protein (3) proved unsuccessful; thus a complete screening for new crystallization conditions was undertaken. Suitable crystals were obtained using the conventional hanging-drop vapor diffusion method under the following conditions: 2 μl of a mother liquor solution containing 1.4 M NaCitrate in 0.1 M HEPES buffer, pH 7.0, were mixed to 2 μl of protein solution concentrated up

[1] Positions are identified topologically following (4).

0006-291X/00 $35.00

TABLE 1

Data Collection, Processing, and Refinement Statistics for *Aply*HT-Mb

Resolution	2.0 Å
Distance crystal-to-detector	100 mm
$\Delta\varphi$	2.0°
number of frames	45
space group	H3
Cell dimensions	a = b = 89.73 Å, c = 92.080 Å $\alpha = \beta = 90.00°$, $\gamma = 120.00°$
R_{merge} (based on intensities)	0.066
Completeness	99.3%
Average I/σ(I)	10.4
R (after rigid body)	0.279
Rfree (after rigid body)	0.297
R (final)	0.189
Rfree (final)	0.215
Number of water molecules	76
Ramachandran plot	
% of residues in most favored regions	97.6
% of residues in additionally allowed regions	2.4
r.m.s.d. from ideality	
main chain bonds (Å)	0.010
main chain angles (°)	2.13

to 30 mg/ml; the resulting droplet was allowed to vapor-equilibrate against 1 ml of mother liquor solution at 294 K. Crystals reached their final dimensions (up to 0.5 × 0.5 × 0.5 mm) in about one month.

Data collection was performed at room temperature using a Rigaku R-AXIS II image-plate detector mounted on a Rigaku rotating anode Cu-kαa X-ray generator equipped with focusing mirrors and working at 50 kV × 100 mA.

*Aply*HT-Mb crystals belong to the hexagonal spacegroup H3 with cell dimensions: a = 89.73 Å, b = 89.73 Å, and c = 92.080 Å with $\alpha = 90.00°$, $\beta = 90.00°$, and $\gamma = 120.00°$. Data were processed with DENZO and scaled and merged with SCALEPACK, both from the HKL package of programs (11). Data collection and processing statistics are summarized in Table 1.

Structure solution and refinement. *Aply*HT-Mb crystallizes under conditions and in a space group different from the native protein. For this reason we used the Molecular Replacement method as implemented in the program A.Mo.Re. (12) to solve the structure. The native *A. limacina* Mb structure (1mba, (3)) was used as a starting model. Considering only one molecule per asymmetric unit, both rotation function and translation function calculations produced clear solutions and were of unambiguous interpretation. Refinement was performed using the Maximum Likelyhood method as implemented in the program REFMAC (12). Each cycle of refining was followed by manual revision of the electron density maps using the X-BUILD/X-AUTOFIT module of the program QUANTA (Molecular Structure Inc.). Water molecules were added only if they had suitable stereochemistry and well defined electron density peaks both on $2F_o$-F_c and F_o-F_c maps, taking care to exclude from the model those waters whose B factor after refinement exceeded 70 Å^2.

The geometrical quality of the model was monitored using the program PROCHECK (12), while structure superposition and r.m.s.d. calculations were performed using the program INSIGHT (Molecular Structure Inc.). Refinement and geometrical statistics on *Aply*HT-Mb structure are summarized in Table 1. Atomic coordinates for *Aply*HT-Mb have been deposited in the Protein Data Bank and the ID accession code is 1DM1.

Binding of azide. Equilibrium constant for azide binding was obtained spectrophotometrically (9), following absorption at 408 nm, using a Cary Varian 50 Probe spectrophotometer. Protein concentration was 4 μM and cuvette path length was set to 1 cm. Kinetics for azide binding were measured by the stopped flow method (9) with an Applied-Photophysics DX-17MV apparatus. All kinetic experiments were carried out in 0.1 M phosphate buffer, pH 7.0, by mixing a solution of met *Aply*HT-Mb with progressively more concentrated sodium azide solutions (protein concentration was 4 μM after mixing). Temperature was 20°C throughout. Absorbance changes were monitored at 408 nm. Under all experimental conditions the observed time course conformed to a single exponential event.

RESULTS AND DISCUSSION

Overall Structure

As expected, the overall structure of *Aply*HT-Mb resembles that of native *Aplysia* Mb purified from the muscle. The r.m.s.d. between Cα for the two structures is 0.411 Å, consistently with the lack of significant secondary structure deviations.

Whereas the N-terminal Ser is acetylated in the native myoglobin, this is not the case for the double mutant expressed in *E. coli* (2). As the acetyl group is well exposed to the solvent (3) and negatively charged, the lack of this group may provide a possible explanation for the failure of *Aply*HT-Mb to crystallize in the same space group as the native protein ($P2_12_12_1$, (3)).

The Heme Pocket

A very interesting feature of Mb from *A. limacina* is the presence of only one His which is at the proximal heme-iron coordination site (F8). The evolutionary conserved distal His is replaced by a Val at topological position E7 (1, 3). In view of the essential role of the distal His(E7) which is absent, an alternative mechanism for stabilization of bound O_2, involving Arg(E10) was proposed (13). Replacing Arg(E10) by Thr (2), dramatically increased the O_2 dissociation rate constant from the value of $k_{off} = 70\ s^{-1}$ of the wt protein to $\approx 700\ s^{-1}$, as well as the autoxidation rate. On the other hand the introduction of an histidyl residue at position E7, both in presence or absence of Arg(E10), had a small effect on O_2 dissociation rate costant ($k > 200\ s^{-1}$), failing to reproduce the value typical of sperm whale Mb ($k = 15\ s^{-1}$), which was proven to depend on the H-bond with the distal His(E7) (14). Therefore trasplantation of the stabilizing interaction typical of mammalian Mbs in the *Aplysia* Mb framework proved to be ineffective.

This observation is now understood on the basis of the crystal structure of the Val(E7)His-Arg(E10)Thr double mutant Mb in the ferric form. The added His(E7) in *Aply*HT-Mb, acquires an atypical "distal" conformation, since the imidazole side chain points away from the iron (Figs. 1 and 2A). The imidazole is stabilized in this open configuration mainly because of the H-bond between the $N_{\epsilon 2}$ of His(E7) and the carbox-

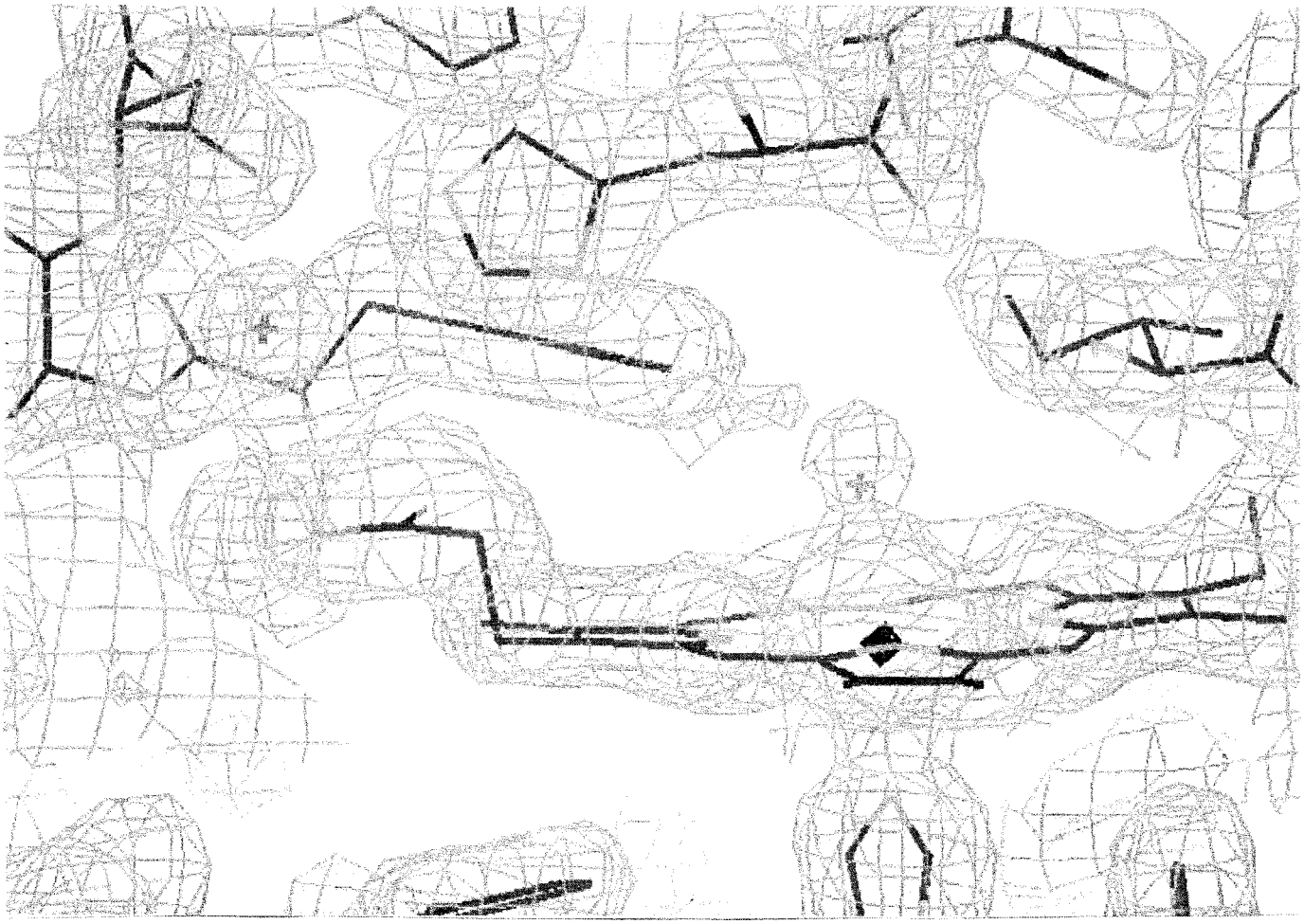

FIG. 1. Electron density map in the heme region of ferric *Aply*HT-Mb contoured at 1.5 σ. The heme is seen edge-on, with the proxymal His(F8) at the bottom, bound to the iron. Two water molecules are shown with a cross; it is evident that the heme iron-coordinated water molecule does not interact with any side chain atom. The His(E7) imidazole does not point toward the heme but interacts with Asp(CD3) carboxylate (upper left corner).

ylate of Asp(CD3), which are at 2.62 Å distance in the crystal structure (Fig. 2A). Moreover the steric hindrance opposed by Phe(CD1) and Ile(E11), which is topologically replaced by a valine in sperm whale Mb, may play a role. As a consequence, the heme pocket in *Aply*HT-Mb is more accessible to the solvent and O_2 dissociation much faster than expected because there is effectively no possibility of a distal H-bond (Figs. 1 and 2A).

In the structure of the ferric ligand-free native *Aplysia* Mb (3, 13), a salt bridge interaction between Arg(E10) and propionate IV has been reported, although the electron density of the side chain of residue Arg(E10) could not be observed. It was presumed that this side chain is disordered out in the solvent, and only upon ligand binding points towards the heme-ligand and acquires order (13). In *Aply*HT-Mb, propionate IV changes its conformation with respect to native Mb as a result of a 180° rotation along the C_{2a}-C_{aa} axis because the salt bridge interaction between Arg(E10) and propionate IV is lost. The open conformation of this propionate also contributes to the increased accessibility of the ligand-binding pocket to the solvent (Fig. 2B).

The optical spectra of the ferric derivative of *A. limacina* wild-type and *Aply*HT-Mb are strikingly different. The maximum of absorption in the Soret region is at 400 nm for both the recombinant *A. limacina* wild-type and the native protein, indicating a high-spin penta-coordinated heme-iron (15); in *Aply*HT-Mb the maximum absorption in the Soret is red-shifted to 408 nm (2). This feature is consistent with the presence of a water molecule in the sixth iron-coordination position as seen from Fig. 1. The same conclusion is reached by examination of the optical spectra in the visible region, where the presence of a peak at 635 nm is indicative of hexa-coordination. Comparison of the spectra measured at pH values of 6.0, 8.0 and 10.0 (i.e. below and

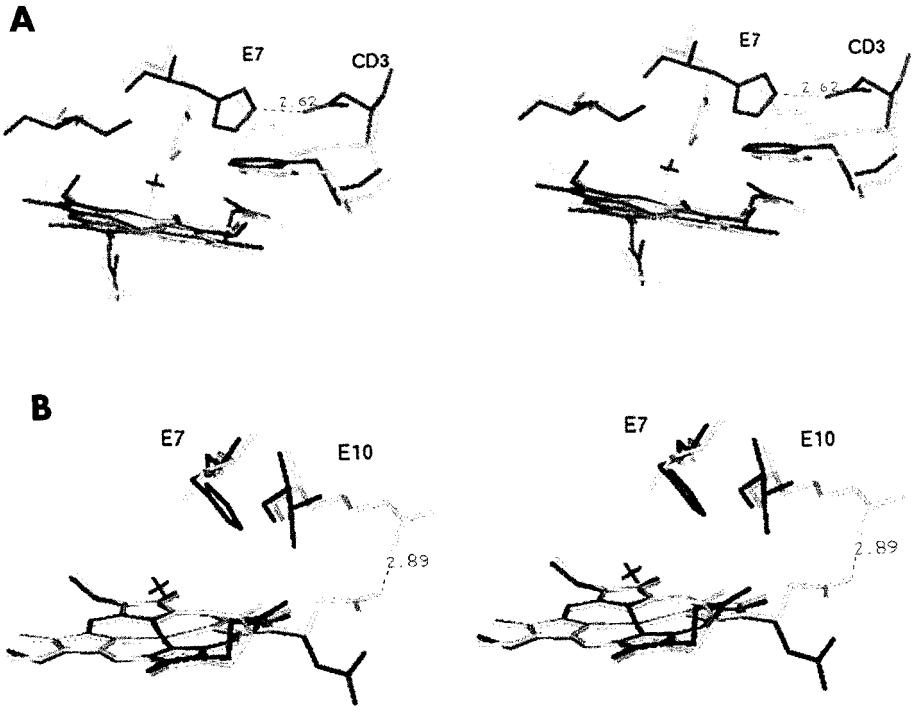

FIG. 2. (A) Stereoview of *Aply*HT-Mb (black) and sperm whale Mb (gray), superimposed. For *Aply*HT-Mb, the orientation of the side chain of His(E7) and its H-bond with Asp(CD3) are highlighted. (B) Stereoview of the structure of the active site of *Aply*HT-Mb (black) and native *A. limacina* Mb (gray), superimposed. The Arg(E10)Thr mutation in *Aply*HT-Mb is responsible for a different orientation of propionate IV.

above the pK of the acid-alkaline transition) indicate that in *Aply*HT-Mb at neutral pH, the sixth coordination position is occupied by a water molecule rather than a hydroxyl ion (data not shown).

To better characterize the stability and the possible role of the H_2O molecule bound to the heme iron of the double mutant *Aply*HT-Mb, we carried out equilibrium and kinetic experiments with azide (Fig. 3). Table 2 presents the relevant parameters for azide binding to the ferric forms of *A. limacina*, *Aply*HT-Mb and sperm whale Mbs. In native *Aplysia* Mb the overall affinity for azide is lower than in sperm whale Mb, mostly because of the very large value of the dissociation rate constant, assigned to the reduced distal interaction due to the absence of His(E7). The larger value of the association rate constant compared to sperm whale Mb is due to a vacant coordination site, because of the absence of a water molecule (15). The new data on the *Aply*HT-Mb mutant are well understood on the basis of the mechanism proposed for azide binding (10). Introduction of the distal residues His(E7) and Thr(E10) in *Aply*HT-Mb has a small but measurable effect on the affinity for azide given that the binding equilibrium constant actually is decreased approximately threefold compared to the wild-type, more significant, however, is the finding that it is still over 30-fold smaller than sperm whale Mb. This observation is fully explained by

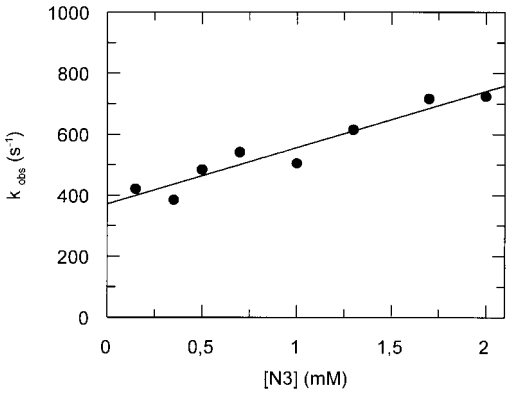

FIG. 3. Dependence on azide concentration of the observed pseudo-first-order rate constant k_{obs}, for the binding to ferric *Aply*HT-Mb, as determined in stopped flow experiments at pH 7.0 and 20°C.

TABLE 2

Equilibrium and Kinetic Constants for Azide Binding

	K (mM^{-1})	k_{on} (mM^{-1} s^{-1})	k_{off} (s^{-1})
Aplysia wild-type[a]	2.5	1800	750
*Aply*HT-Mb	0.9	184	204[b], 371[c]
Sperm whale Mb[a]	29	2.9	0.1

[a] From (16).
[b] Calculated from k_{on} and K.
[c] As determined by the intercept on the y axis of the linear fit shown in Fig. 3.

the orientation of His(E7) side chain, which points out of the distal pocket therefore failing to stabilize the bound ligand through an H-bond. The mechanism of azide association to met-Mb is complex and is governed by different factors including primarily steric hindrance of the distal pocket and displacement of a coordinated water molecule (10). The tenfold reduction of the association rate constant calculated for *Aply*HT-Mb (see Fig. 3 and Table 2) with respect to *A. limacina* wild-type is consistent with the presence of a coordinated water molecule to be displaced, which is clearly visible in *Aply*HT-Mb structure: a B-factor value of 33 $Å^2$ for the water oxygen and a distance of 2.37 Å from the heme-iron have been determined after refinement. However since this water molecule is not stabilized by a distal H-bond (because of the configuration of His(E7)), the rate constant for azide binding in *Aply*HT-Mb is still 50 fold faster than that of sperm whale Mb, mainly because His(E7) cannot exert its putative role as a "gate" to modulate azide entry (10). Along the same lines, we can semiquantitatively explain the trend shown by the azide dissociation rate constant (see Table 2), given that the lack of favorable charge interaction accellerates dissociation compared to sperm whale Mb, because of the odd stereochemistry of the newly introduced His(E7) in *Aply*HT-Mb.

CONCLUSIONS

The *Aply*HT-Mb mutant was prepared and characterized with the following purposes in mind. First of all, we wanted to obtain some direct evidence for the hypothesis that in Mbs lacking the distal His(E7), an alternative mechanism for O_2 stabilization is possible. In *A. limacina* Mb, O_2 stabilization was proposed (7) to be provided by a residue located at a different topological position, i.e. Arg(E10) switching back into the heme pocket to stabilize the iron-bound ligand. Moreover we aimed at reproducing the exact O_2 binding parameters of sperm whale Mb in the *A. limacina* Mb framework by replacing the Val(E7) and Arg(E10) residues, peculiar of *A. limacina* Mb, with the topologically corresponding residues of the mammalian Mbs, i.e. His and Thr. The O_2 dissociation and the autooxidation rate constants for the two mutants, clearly demonstrate that Arg(E10) is involved in O_2 stabilization, thus providing a direct confirmation to the above hypothesis (2, 7). However, our attempt to reproduce the critical H-bond on the distal site by introducing His(E7) in *A. limacina* Mb was unsuccessful, as witnessed by the fact that the O_2 dissociation rate constant of this mutant is much faster than either sperm whale Mb or *A. limacina* Mb. The crystal structure of the ferric *Aply*HT-Mb double mutant provides an explanation for the kinetic and spectroscopic data. It is clear from Fig. 1 that His(E7) added by mutagenesis cannot take the side chain conformation required for ligand stabilization, partially as a result of steric hindrance opposed by nearby residues, but mainly as a consequence of a newly established H-bond with Asp(CD3). This interaction can not take place in sperm whale Mb where the residue at topological position CD3 is Arg; thus we expect that a new mutant with Asp(CD3) replaced by a nonpolar or positively charged residue, may have the distal His in a productive conformation, possibly reproducing the sperm whale Mb rate constant. The presence of a water molecule bound to the sixth coordination position of the ferric form of *Aply*HT-Mb, previously suggested on the basis of spectroscopic evidence (2) is proven by the X-ray structure (Fig. 1). However the azide binding data show that this water, though coordinated, is quite labile, as shown particularly by the relatively high value of the second order combination rate constant for complex formation with azide (shown as k_{on} in Table 2). On the basis of structural evidences, therefore the kinetic results are rationalized in terms of increased accessibility to the ligand binding pocket, a direct consequence of the substitution of Arg(E10) imposing a new conformation for the corresponding heme-propionate (Fig. 3), as well as to the presence of a water molecule at the sixth iron-coordination position, which is absent in the native *A. limacina* Mb and present in *Aply*HT-Mb though weakly bound because of the open configuration of the newly introduced His(E7).

ACKNOWLEDGMENTS

We thank Dr. L. Nicolini and Mr. R Dagai (Istituo Superiore di Sanità, Rome, Italy) for large-scale growth of bacterial cells for protein purification. Funds from C.N.R. (No. 97.04083.CT04) are gratefully acknowledged.

REFERENCES

1. Tentori, L., Vivaldi, G., Carta, S., Marinucci, M., Massa, M., Antonini, E., and Brunori, M. (1971) *FEBS Lett.* **12,** 181–186.
2. Cutruzzolà, F., Travaglini-Allocatelli, C., Brancaccio, A., and Brunori, M. (1996) *Biochem. J.* **314,** 83–90.
3. Bolognesi, M., Onesti, S., Gatti, G., Coda, A., Ascenzi, P., and Brunori, M. (1989) *J. Mol. Biol.* **205,** 529–544.
4. Kendrew, J. C., Dickerson, R. E., Strandberg, B. E., Hart, R. E, Davies, D. R., Philips, D. C., and Shore, V. C. (1960) *Nature* **185,** 422.
5. Perutz, M. F. (1989) *Trends Biochem. Sci.* **14,** 42–44.
6. Springer, B. A., Sligar, S. G., Olson, J. S., and Phillips, G. N., Jr. (1994) *Chem. Rev.* **94,** 699–714.
7. Bolognesi, M., Coda, A., Frigerio, F., Gatti, G., Ascenzi, P., and Brunori, M. (1990) *J. Mol. Biol.* **151,** 315–319.
8. Wittenberg, B. A., Brunori, M., Antonini, E., Wittenberg, J. B., and Wyman, J. (1965) *Arch. Biochem. Biophys.* **111,** 576–579.
9. Antonini, E., and Brunori, M. (1971) Hemoglobin and Myoglobin in Their Reactions with Ligands, North-Holland Publishing Co., Amsterdam.
10. Brancaccio, A., Cutruzzolà, F., Travaglini-Allocatelli, C.,

Brunori, M., Smerdon, S. J., Wilkinson, A. J., Dou, Y., Keenan, D., Ikeda-Saito, M., Brantley, R. E., Jr., and Olson, J. S. (1994) *J. Biol. Chem.* **269,** 13843–13853.

11. Otwinoski, Z., and Minor W. (1997) *Methods Enzymol.* **276,** 307–326.
12. Collaborative Computing Project No. 4. (1994) *Acta Cryst.* **D50,** 760–763.
13. Conti, E., Moser, C., Rizzi, M., Mattevi, A., Lionetti, C., Coda, A., Ascenzi, P., Brunori, M., and Bolognesi, M. (1993) *J. Mol. Biol.* **233,** 498–508.
14. Olson, J. S., Mathews, A. J., Rohlfs, R. J., Springer, B. A., Egeberg, K. D., Sligar S. J., Tame, J., Renaud, J., and Nagai, K. (1988) *Nature* **336,** 265–266.
15. Giacometti, G. M., Ascenzi, P., Brunori, M., Rigatti, G., and Bolognesi, M. (1981) *J. Mol. Biol.* **151,** 315–319.
16. Smerdon, S. J., Krzywda, S., Brzozowski, A. M., Davies, G. J., Wilkinson, A. J., Brancaccio, A., Cutruzzolà, F., Travaglini-Allocatelli, C., Brunori, M., Tiansheng, L., Brantley, R. E., Jr., Carver, T. E., Eich, R. F., Singleton, E., and Olson, J. S. (1995) *Biochemistry* **34,** 8715–8725.